Differential Semblance Velocity Analysis by Reverse Time Migration: Image Gathers and Theory

Fuchun Gao, Total, William Symes, Rice University

Summary

Velocity models can be automatically updated by differential semblance velocity analysis (DSVA). To overcome the dip limitations associated with the one-way wave equation based imaging algorithms, we propose in this study that the common image gathers can be defined other than in horizontal offset domain within the reverse time migration(RTM) framework, where two-way wave equation is solved as the wave propagator. A function to be minimized in differential semblance analysis is set up and the principle in DSVA is verified in this study that the velocity is correct when the function is minimized. We also show a detailed derivation of an algorithm that the velocity model can be updated automatically through the differential semblance analysis in the RTM frame work.

Introduction

A good velocity model is important in the sense that the quality of final migration image depends on it. As the imaging tools evolve from ray-based, to one-way wave equation based, and finally to the two-way wave-equation based reverse time migration, the velocity model plays even more important role in imaging because the advantage of more sophisticated migration algorithms is evident only when the velocity model is reliable. On the other hand, ray-based reflection tomography is still the most widely applied velocity modeling method in the energy industry. The muiti-pathing effect in wave propagation can cause problems in such practices because the common image gathers may not be flat even when the velocity is correct (e.g., Nolan and Symes, 1996). Flattening of common image gathers is relatively efficient using the ray-based reflection tomography. However, such methods require extensively event picking before the tomography, which is generally time-consuming.

In the past a few years, it has been found that velocity models can indeed be automatically updated based on the differential semblance methods (e.g., Shen and Symes, 2008; Foss et al., 2004; Shen et al., 2003; Mulder and ten Kroode, 2002). While the principle of focusing images in these methods is the same as that in the conventional reflection tomography, the velocity model is updated automatically by minimizing the mean square of the image volume scaled by offset in the subsurface domain. The image volumes are generated by one-way wave equation migrations, which generally produce more artifact-free common image gathers that do Kirchhoff type migrations (Stolk and Symes, 2004; de Hoop and Stolk, 2006).

More recently, with the progress in computing hardware and in forward modeling algorithms, reverse time migration (RTM) has become an effective imaging tool in the energy industry. One advantage of RTM is that it overcomes the steep dip limitation shown in the one-way wave equation based migrations. Conventionally the sub-surface gathers are usually defined in horizontal offsets, but with RTM, gathers can go beyond that (Biondi and Shan, 2002; Biondi and Symes, 2004). In this paper, we describe the construction of both horizontal and vertical offset image gathers using reverse time migration implemented in the frequency domain. The DSVA principle remains valid for these generalized common image gathers. Therefore, we can develop an algorithm of differential semblance velocity analysis under the RTM framework.

This paper first provides a general theoretical background of the common image gathers defined in the horizontal offset domain as well as in vertical offset domain. Examples of these gathers in different settings are shown. Secondly, this paper shows the detailed derivation of how the velocity analysis can be performed utilizing the differential semblance frame work by solving the two-way wave equation.

Theoretical background

The first part of this section covers the theoretical background on how the common image gathers can be constructed in the horizontal offset domain as well in the vertical offset domain. The second part covers a theoretical derivation for the DSVA in RTM framework, showing the definition of the object function and its derivative with respect to the model parameter, i.e., seismic velocity. All derivations are in 2D and in matrix format.

Horizontal and Vertical Offset Common Image Gather

The horizontal offset common image gather (HOCIG) is defined as

$$\mathbf{I}(z,h,\omega)\,|_{x=x0} = \mathbf{u}(x+h,z,\omega)\mathbf{v}(x-h,z,\omega) \qquad (1),$$

where h is the horizontal offset, $\mathbf{u}$ and $\mathbf{v}$ are the forward modeled and back-propagated wave fields determined by solving the acoustic wave equation in frequency-space domain:

$$S\,\mathbf{u} = \mathbf{f} \quad \text{and} \quad S\,\mathbf{v} = -\mathbf{d}^{*} \qquad (2),$$

where S is the impedance matrix, $\mathbf{u}$ and $\mathbf{v}$ are the forward modeled and back-propagated wave fields to be determined. $\mathbf{f}$ and $\mathbf{d}$ are source signatures and the observed data treated as sources in frequency domain. * denotes conjugate. Details of frequency-space domain forward modeling can be seen in Pratt et al. (1998).

Since full acoustic waves are solved here, vertical offset common image gathers (VOCIG) can also be defined:

$$\mathbf{I}(x,h,\omega)\,|_{z=z0} = \mathbf{u}(x,z+h,\omega)\mathbf{v}(x,z-h,\omega) \qquad (3).$$

Time domain image gathers can be readily synthesized by summing up all the frequency domain gathers. One property of the common image gathers defined here is that if the velocity is correct, most energy should concentrate at the zero offset and otherwise the energy will scattered into non-zero offset.

Differential semblance velocity analysis

In the differential semblance velocity analysis, the velocity can be updated by making use of the property the CIG has that the velocity is correct when the energy in CIGs concentrates around the zero offset. First, we define a new semblance weighted by offset

$$\bar{\mathbf{I}} = \mathrm{h}\mathbf{I} \qquad (4),$$

where h is the offset in either the HOCIG or VOCIG and $\mathbf{I}$ is the image gather defined in Equations (1) and (3). In matrix convention, the semblance weighted by offset can be expressed as a column vector

$$\bar{\mathbf{I}} = \begin{pmatrix} \mathrm{h}_1\mathrm{u}_1\mathrm{v}_1 \\ \vdots \\ \mathrm{h}_n\mathrm{u}_n\mathrm{v}_n \end{pmatrix} \qquad (5),$$

which is called the weighted common image vector.

In DSVA, velocity model can be updated iteratively by minimizing the object function defined as

$$\mathrm{J} = \frac{1}{2}\bar{\mathbf{I}}^{\mathrm{t}}\bar{\mathbf{I}}^{*} \qquad (6),$$

where ^{t} denotes transpose and * denotes conjugate.

The first step in adjoint analysis is to formulate the perturbation in object function as a linear function of the perturbation in model parameters. This is usually done under Born approximation.

$$\mathrm{F}\delta\mathbf{c} = \delta\mathrm{J} = \frac{\partial \mathrm{J}}{\partial \mathbf{c}}\delta\mathbf{c} = \mathrm{Re}\left\{\left(\frac{\partial \bar{\mathbf{I}}}{\partial \mathbf{c}}\right)^{\mathrm{t}}\bar{\mathbf{I}}^{*}\right\}\delta\mathbf{c} \qquad (7).$$

where F is an operator which maps the perturbation in model parameter to the perturbation in the object function. So we need to compute the derivative of the weighted common image vector with respect to the velocity vector $\mathbf{c}$.

$$\frac{\partial \mathbf{I}}{\partial \mathbf{c}} = \begin{bmatrix} \mathrm{h}_1(\frac{\partial \mathrm{u}_1}{\partial \mathbf{c}}\mathrm{v}_1 + \mathrm{u}_1\frac{\partial \mathrm{v}_1}{\partial \mathbf{c}}) \\ \mathrm{h}_2(\frac{\partial \mathrm{u}_2}{\partial \mathbf{c}}\mathrm{v}_2 + \mathrm{u}_2\frac{\partial \mathrm{v}_2}{\partial \mathbf{c}}) \\ \vdots \\ \mathrm{h}_n(\frac{\partial \mathrm{u}_n}{\partial \mathbf{c}}\mathrm{v}_n + \mathrm{u}_n\frac{\partial \mathrm{v}_n}{\partial \mathbf{c}}) \end{bmatrix} = \begin{bmatrix} \mathrm{hv}_1 \\ \mathrm{hv}_2 \\ \vdots \\ \mathrm{hv}_n \end{bmatrix} .* \begin{bmatrix} \frac{\partial \mathrm{u}_1}{\partial \mathbf{c}} \\ \frac{\partial \mathrm{u}_2}{\partial \mathbf{c}} \\ \vdots \\ \frac{\partial \mathrm{u}_n}{\partial \mathbf{c}} \end{bmatrix} + \begin{bmatrix} \mathrm{hu}_1 \\ \mathrm{hu}_2 \\ \vdots \\ \mathrm{hu}_n \end{bmatrix} .* \begin{bmatrix} \frac{\partial \mathrm{v}_1}{\partial \mathbf{c}} \\ \frac{\partial \mathrm{v}_2}{\partial \mathbf{c}} \\ \vdots \\ \frac{\partial \mathrm{v}_n}{\partial \mathbf{c}} \end{bmatrix}$$

$$= \begin{bmatrix} \mathrm{h}_1\mathrm{v}_1 & \mathrm{h}_1\mathrm{v}_1 & \cdots & \mathrm{h}_1\mathrm{v}_1 \\ \mathrm{h}_2\mathrm{v}_2 & \mathrm{h}_2\mathrm{v}_2 & \cdots & \mathrm{h}_2\mathrm{v}_2 \\ \vdots & \vdots & \vdots & \vdots \\ \mathrm{h}_n\mathrm{v}_n & \mathrm{h}_n\mathrm{v}_n & \cdots & \mathrm{h}_n\mathrm{v}_n \end{bmatrix} .* \begin{bmatrix} \frac{\partial \mathrm{u}_1}{\partial \mathrm{c}_1} & \frac{\partial \mathrm{u}_1}{\partial \mathrm{c}_2} & \cdots & \frac{\partial \mathrm{u}_1}{\partial \mathrm{c}_m} \\ \frac{\partial \mathrm{u}_2}{\partial \mathrm{c}_1} & \frac{\partial \mathrm{u}_2}{\partial \mathrm{c}_2} & \cdots & \frac{\partial \mathrm{u}_2}{\partial \mathrm{c}_m} \\ \vdots & \vdots & \vdots & \vdots \\ \frac{\partial \mathrm{u}_n}{\partial \mathrm{c}_1} & \frac{\partial \mathrm{u}_n}{\partial \mathrm{c}_2} & \cdots & \frac{\partial \mathrm{u}_n}{\partial \mathrm{c}_m} \end{bmatrix} +$$

$$\begin{bmatrix} \mathrm{h}_1\mathrm{u}_1 & \mathrm{h}_1\mathrm{u}_1 & \cdots & \mathrm{h}_1\mathrm{u}_1 \\ \mathrm{h}_2\mathrm{u}_2 & \mathrm{h}_2\mathrm{u}_2 & \cdots & \mathrm{h}_2\mathrm{u}_2 \\ \vdots & \vdots & \vdots & \vdots \\ \mathrm{h}_n\mathrm{u}_n & \mathrm{h}_n\mathrm{u}_n & \cdots & \mathrm{h}_n\mathrm{u}_n \end{bmatrix} .* \begin{bmatrix} \frac{\partial \mathrm{v}_1}{\partial \mathrm{c}_1} & \frac{\partial \mathrm{v}_1}{\partial \mathrm{c}_2} & \cdots & \frac{\partial \mathrm{v}_1}{\partial \mathrm{c}_m} \\ \frac{\partial \mathrm{v}_2}{\partial \mathrm{c}_1} & \frac{\partial \mathrm{v}_2}{\partial \mathrm{c}_2} & \cdots & \frac{\partial \mathrm{v}_2}{\partial \mathrm{c}_m} \\ \vdots & \vdots & \vdots & \vdots \\ \frac{\partial \mathrm{v}_n}{\partial \mathrm{c}_1} & \frac{\partial \mathrm{v}_n}{\partial \mathrm{c}_2} & \cdots & \frac{\partial \mathrm{v}_n}{\partial \mathrm{c}_m} \end{bmatrix}$$

$$= \begin{bmatrix} \mathbf{q}_1 & \mathbf{q}_1 & \cdots & \mathbf{q}_1 \end{bmatrix} * \frac{\partial \mathbf{u}}{\partial \mathbf{c}} + \begin{bmatrix} \mathbf{q}_2 & \mathbf{q}_2 & \cdots & \mathbf{q}_2 \end{bmatrix} * \frac{\partial \mathbf{v}}{\partial \mathbf{c}}$$

$$= \mathrm{H}_1 .* \frac{\partial \mathbf{u}}{\partial \mathbf{c}} + \mathrm{H}_2 .* \frac{\partial \mathbf{v}}{\partial \mathbf{c}} \qquad (8),$$

where $\mathbf{q}_1 = \begin{bmatrix} \mathrm{h}_1\mathrm{v}_1 \\ \mathrm{h}_2\mathrm{v}_2 \\ \vdots \\ \mathrm{h}_n\mathrm{v}_n \end{bmatrix}$ and $\mathbf{q}_2 = \begin{bmatrix} \mathrm{h}_1\mathrm{u}_1 \\ \mathrm{h}_2\mathrm{u}_2 \\ \vdots \\ \mathrm{h}_n\mathrm{u}_n \end{bmatrix}$. The symbol .* denotes array multiplication (not matrix multiplication), i.e., the corresponding elements are multiplied. $\frac{\partial \mathbf{u}}{\partial \mathbf{c}}$ and $\frac{\partial \mathbf{v}}{\partial \mathbf{c}}$ are the derivatives of wave fields with respect to model parameters which are commonly called Frechet kernels. The above derivation shows that $\frac{\partial \bar{\mathbf{I}}}{\partial \mathbf{c}}$ can be determined as the sum of two correlations between the two kernels and two respective wave fields.

By taking derivative with respect to velocity on both sides if equation (2), we get

$$\mathrm{S}\frac{\partial \mathbf{u}}{\partial \mathrm{c_i}} = -\frac{\partial \mathrm{S}}{\partial \mathrm{c_i}}\mathbf{u} = \mathbf{f}^{(\mathrm{i})} \qquad \text{or} \qquad \frac{\partial \mathbf{u}}{\partial \mathbf{c}} = \mathrm{S}^{-1}\mathrm{F_1} \qquad (9),$$

where $F_1 = \left[f^{(1)} \; f^{(2)} \cdots f^{(m)} \right]$, where m is the number of model parameters. To compute the Frechet kernels explicitly, each would require m forward solutions which is a forbidding task. The following is a derivation to avoid computing them explicitly. Introducing Equation (6) into Equation (5), we have

$$\begin{aligned} \frac{\partial \mathbf{I}}{\partial \mathbf{c}} &= \mathrm{H}_1 .* \frac{\partial \mathbf{u}}{\partial \mathbf{c}} + \mathrm{H}_2 .* \frac{\partial \mathbf{v}}{\partial \mathbf{c}} \qquad (10). \\ &= \mathrm{H}_1 .* (\mathrm{S}^{-1}\mathrm{F}_1) + \mathrm{H}_2 .* (\mathrm{S}^{-1}\mathrm{F}_2) \end{aligned}$$

Therefore Equation (7) becomes

$$\begin{aligned} \mathrm{F}\delta\mathbf{c} = \delta \mathrm{J} &= \mathrm{Re}\left\{ \left(\frac{\partial \bar{\mathbf{I}}}{\partial \mathbf{c}} \right)^{\mathrm{t}} \bar{\mathbf{I}}^{*} \right\} \delta\mathbf{c} \\ &= \mathrm{Re}\left\{ \{\mathrm{H}_1^{\mathrm{t}} .* [\mathrm{F}_1^{\mathrm{t}} (\mathrm{S}^{-1})^{\mathrm{t}}]\} \bar{\mathbf{I}}^{*} + \{\mathrm{H}_2^{\mathrm{t}} .* [\mathrm{F}_2^{\mathrm{t}} (\mathrm{S}^{-1})^{\mathrm{t}}]\} \bar{\mathbf{I}}^{*} \right\} \delta\mathbf{c} \\ &= \mathrm{Re}\left\{ \mathrm{F}_1^{\mathrm{t}} (\mathrm{S}^{-1})^{\mathrm{t}} (\mathbf{q}_1 .* \bar{\mathbf{I}}^{*}) + \mathrm{F}_2^{\mathrm{t}} (\mathrm{S}^{-1})^{\mathrm{t}} (\mathbf{q}_2 .* \bar{\mathbf{I}}^{*}) \right\} \delta\mathbf{c} \\ &= \mathrm{Re}\left\{ \mathrm{F}_1^{\mathrm{t}} (\mathrm{S}^{-1})^{\mathrm{t}} \hat{\mathbf{I}}_1 + \mathrm{F}_2^{\mathrm{t}} (\mathrm{S}^{-1})^{\mathrm{t}} \hat{\mathbf{I}}_2 \right\} \delta\mathbf{c} \\ &= \mathrm{Re}\left\{ \mathrm{F}_1^{\mathrm{t}} \mathrm{W}_1 + \mathrm{F}_2^{\mathrm{t}} \mathrm{W}_2 \right\} \delta\mathbf{c} \end{aligned}$$

where $\hat{\mathbf{I}}_1 = \mathbf{q}_1 .* \bar{\mathbf{I}}^{*}$ and $\hat{\mathbf{I}}_2 = \mathbf{q}_2 .* \bar{\mathbf{I}}^{*}$ are the correlation of CIGs with the forward modeled and back-propagated wave fields. These two vectors can be treated as two virtual sources. $\mathrm{W}_1 = (\mathrm{S}^{-1})^{\mathrm{t}} \hat{\mathbf{I}}_1$ and $\mathrm{W}_2 = (\mathrm{S}^{-1})^{\mathrm{t}} \hat{\mathbf{I}}_2$ are the wave fields determined by propagating the two virtual sources. Therefore, the operator F is simply

$$\mathrm{F} = \mathrm{F}_1^{\mathrm{t}} \mathrm{W}_1 + \mathrm{F}_2^{\mathrm{t}} \mathrm{W}_2 \qquad (11).$$

The adjoint operator of it is simply the transpose of it. The DS optimization problem can be solved by the SVL software package available at TRIP group of Rice University once the operator and adjoint operator are ready.

Examples

To validate the fundamental concept in DSVA that the energy concentrates in the zero offset if the velocity is true in the reverse time migration framework, we first set up a simple synthetic model (Figure 1) to construct CIG gathers in frequency as well as in time domain and to monitor the variation of the objective function as velocity changes.

Figure 2 shows the real part of the CIG gathers in frequency domain. It can be seen in the figure that no matter how it is different from frequency to frequency, the energy concentrates around the zero offset for all frequencies at true velocity. The time domain CIGs can be synthesized from the frequency domain CIGs (Figure 3) and they behave in the same principle. The objective function (bottom plot of Figure 3) to be minimized is truly in convex shape. The simple test show that the velocity is true as expected if the object function is at the minimum.

Within the RTM framework, the CIGs can even be defined beyond the conventional vertical symmetrical axis with horizontal offsets. Figure 4 shows a synthetic model with a vertical discontinuity in a background velocity model where velocity linearly increases with depth. The common image gathers can be even defined versus a horizontal axis with vertical offset, which are shown in Figure 5.

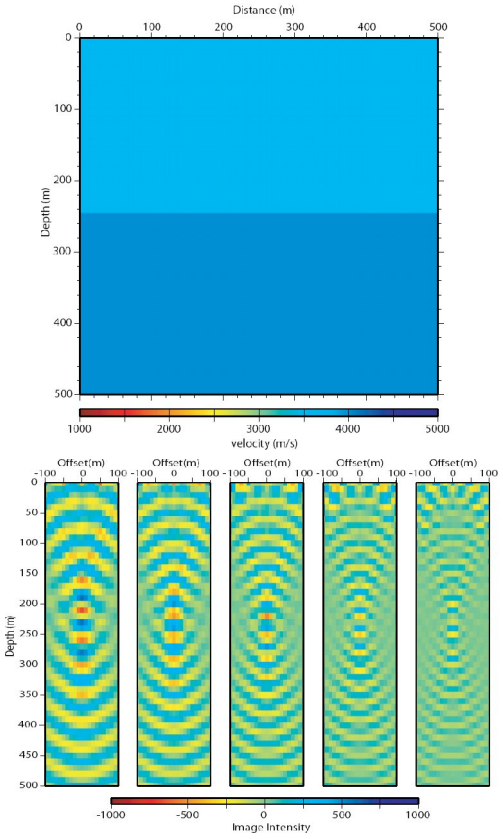

Figure 1. The synthetic model and frequency domain CIGs at X=300.0m from 40 to 72Hz.

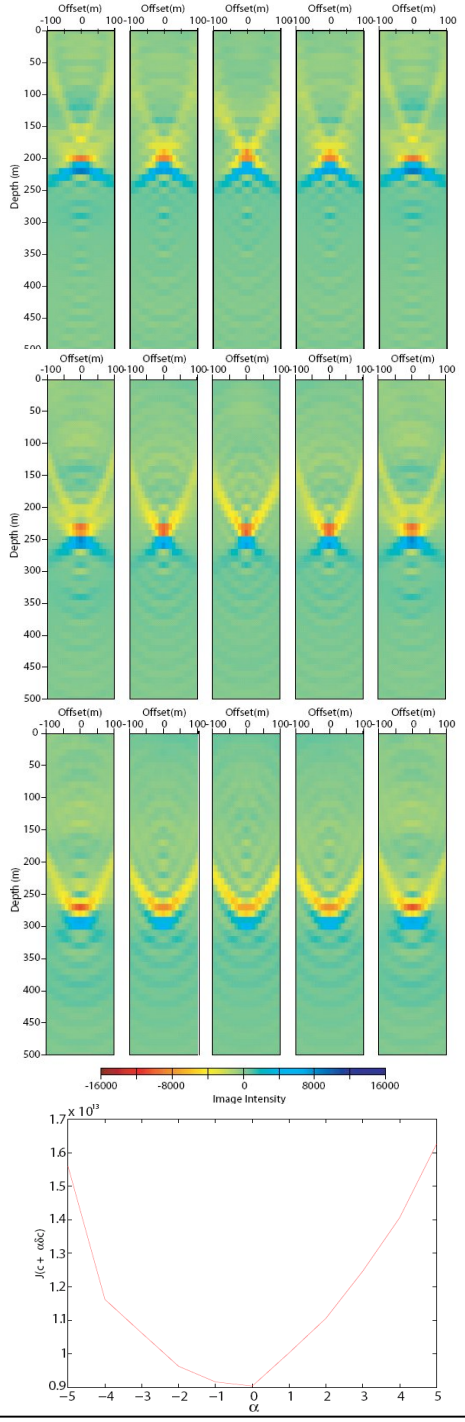

Figure 3. Five time domain CIGs at different velocities, 3.0km/s (top), 3.5km/s (second) and 4.0km/s (third), and the magnitude of the object function versus perturbation coefficients(bottom). The velocity perturbation is 100m/s.

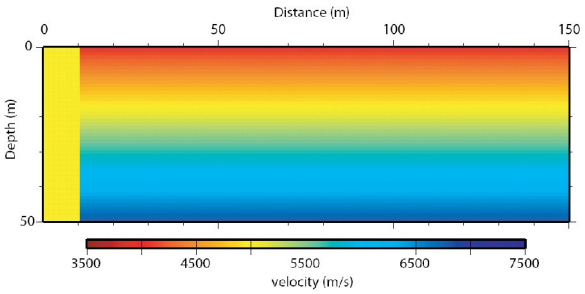

Figure 4. The synthetic velocity model for the vertical offset CIG test.

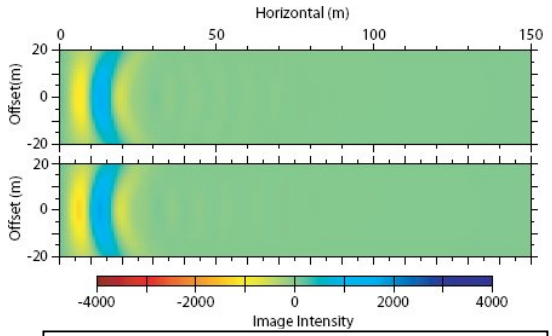

Figure 5. Vertical offset CIG (VOCIG) at two locations z=30m and z=35m.

Discussion and Conclusion

It is proposed to do velocity analysis for migration though differential semblance within the reverse time migration framework. This study is the initial part toward that goal. We can see that the common image gathers can be formed in frequency domain and be synthesized into time domain if necessary. It is confirmed in this study that within the RTM framework, the object function to be minimized in the differential semblance analysis is in convex shape and the velocity is correct when the minimum of the function is reached. The theoretical frame work for DSVA is derived in this study and will be the foundation for following studies.

The physical interpretation of the adjoint operator and the velocity updating will be reported in following separate studies.

Acknowledgements

We sincerely thank Prof. Gerhard Pratt for discussions on the work in this study. The second author is grateful to the sponsors of The Rice Inversion Project for their continuing support of this research.

EDITED REFERENCES

Note: This reference list is a copy-edited version of the reference list submitted by the author. Reference lists for the 2009 SEG Technical Program Expanded Abstracts have been copy edited so that references provided with the online metadata for each paper will achieve a high degree of linking to cited sources that appear on the Web.

REFERENCES

Biondi, B., and G. Shan, 2002, Prestack imaging of overturned reflection by reverse time migration: 72nd Annual International Meeting, SEG, Expanded Abstracts, 1284–1287.

Biondi, B., and W. Symes, 2004, Angle-domain common image gathers for migration velocity analysis by wavefield continuation imaging: Geophysics, **67**, 1283–1298.

de Hoop, M. V., and C. Stolk, 2006, Seismic inverse scattering in the down-ward continuation approach: Wave Motion, **43**, 579–598.

Foss, S. K., B. Ursin, and M. V. de Hoop, 2004. Depth-consistent p- and s-wave velocity reflection tomography using pp and ps seismic data: 74th Annual International Meeting, SEG, Expanded Abstracts, 2363–2367.

Mulder, W., and A. ten Kroode, 2002, Automatic velocity analysis by differential semblance optimization: Geophysics, **67**, 1184–1191.

Nolan, C., and W. W. Symes, 1996, Imaging in complex velocities with general acquisition geometry: TRIP, The Rice Inversion Project, Technical Report.

Pratt, G., C. S. Shin, and G. J. Hicks, 1998, Gauss-Newton and full Newton methods in frequency-domain seismic waveform inversion: Geophysical Journal International, **133**, 341–362.

Shen, P., C. Stolk, and W. Symes, 2003, Automatic velocity analysis by differential semblance optimization: 73rd Annual International Meeting, SEG, Expanded Abstracts, 2132–2135.

Shen, P., and W. W. Symes, 2008, Automatic velocity analysis via shot profile migration: Geophysics, **73**, no. 5, VE49–VE59.

Stolk, C., and W. Symes, 2004, Kinematic artifacts in prestack depth migration: Geophysics, **69**, 562–575.

Symes, W. W., 1993, A differential semblance criterion for inversion of multioffset seismic reflection data: Journal of Geophysical Research, **98**, 2061–2073.